Dalton Transactions

PAPER

View Article Online
View Journal | View Issue

Cite this: *Dalton Trans.*, 2016, **45**, 17662

Assessment of the nematocidal activity of metallocenyl analogues of monepantel†

Jeannine Hess,[a] Malay Patra,[a] Abdul Jabbar,[b] Vanessa Pierroz,[a,c] Sandro Konatschnig,[a] Bernhard Spingler,[a] Stefano Ferrari,[c] Robin B. Gasser*[b] and Gilles Gasser*‡[a]

In this study, we present the design, synthesis, characterization and biological evaluation of structurally new ferrocenyl and ruthenocenyl derivatives of the organic anthelmintic monepantel (Zolvix®). All seven metallocenyl derivatives prepared (**4a**/**b**, **5a**/**b**, **6a**/**b** and **7**) were isolated as racemates and characterized by ^{1}H, ^{13}C and ^{19}F NMR spectroscopies, mass spectrometry, IR spectroscopy and elemental microanalysis. The molecular structures of four compounds (**4a**/**b**, **6a** and **7**) were further confirmed by X-ray crystallography. The biological activities of the organometallic intermediates (**4a**/**b**) and organometallic derivatives of monepantel (**5a**/**b**, **6a**/**b** and **7**) were evaluated *in vitro* using parasitic nematodes of major importance in livestock, namely *Haemonchus contortus* and *Trichostrongylus colubriformis*. Two ferrocenyl compounds (**4a** and **6a**) showed nematocidal activity, while the analogous ruthenocenyl compounds (**4b** and **6b**) were not active at the highest concentration tested (10 μg mL^{-1}). In order to obtain insight into the difference in activity between ferrocenyl and ruthenocenyl derivatives, the potential of the compounds for reactive oxidative species (ROS) production in live cells was assessed. Interestingly, neither the ferrocenyl nor the ruthenocenyl compounds (**4a**/**b** and **6a**/**b**) produced significant ROS in HeLa cells when checked after 22 h, potentially indicating a redox-independent activity of **4a** and **6a** on the parasites. The selectivity of the compounds on parasites was confirmed by investigating their cytotoxicity profiles. None of these compounds was toxic either to HeLa or MRC-5 cells. Thus, **4a** and **6a** could be considered as interesting leads for further development of new classes of anti-parasitic agents.

Received 29th August 2016,
Accepted 3rd October 2016

DOI: 10.1039/c6dt03376h

www.rsc.org/dalton

Introduction

The impact of parasitic diseases on animals and humans is substantial around the world. Controlling parasites of domesticated animals is a major issue, and usually relies exclusively on chemotherapy with an arsenal of broad-spectrum anthelmintics.[2,3] The excessive use of these drugs has resulted in the emergence of resistance, and multi-drug resistant parasites are now widespread.[5–8] Apart from the classical groups of anthelmintics, such as the benzimidazoles, imidazothiazoles and macrocyclic lactones, a new synthetic anthelmintic class, the amino-acetonitrile derivatives (AADs, see Scheme 1), has been discovered, and a promising candidate of this class, called monepantel (AAD 1566), was recently commercialized.[1,9,10]

Investigations have shown that the safety profile of monepantel relates to its target, a nematode specific nicotinic acetylcholine receptor (nAChr) subunit, which is absent in host mammals.[11–13] Although monepantel now represents a new class of anthelmintic drug, unfortunately, some years after its introduction and use in the field, nematodes with reduced sensitivity to monepantel have been detected in several countries including Uruguay, New Zealand and Brazil.[14–18] Given this rapid emergence of resistance to monepantel, there is an urgent need to develop novel and superior control strategies to ensure the sustainability of parasite control. With this in mind, our group recently started to derivatize monepantel

[a]*Department of Chemistry, University of Zurich, Winterthurerstrasse 190, CH-8057 Zurich, Switzerland. E-mail: gilles.gasser@chimie-paristech.fr; http://www.gassergroup.com*
[b]*Faculty of Veterinary and Agricultural Sciences, The University of Melbourne, Parkville, Victoria 3010, Australia. E-mail: robinbg@unimelb.edu.au; http://www.gasserlab.org/; Tel: +61 3 9731 2283*
[c]*Institute of Molecular Cancer Research, University of Zurich, Winterthurerstrasse 190, CH-8057 Zurich, Switzerland*

†Electronic supplementary information (ESI) available: ^{1}H, ^{13}C and ^{19}F NMR spectra (**4a**/**b**, **5a**/**b**, **6a**/**b** and **7**) (Fig. S1–S16), ORTEP plot of **7** (Fig. S17), anti-parasitic activity against *C. felis*, *L. cuprina* and *R. sanguineus* of organometallic precursors and derivatives (**4a**/**b**, **5a**/**b**, **6a**/**b** and **7**) (Table S1). CCDC 1501422–1501425. For ESI and crystallographic data in CIF or other electronic format see DOI: 10.1039/c6dt03376h

‡Present address: Chimie ParisTech, PSL Research University, 11, rue Pierre et Marie Curie, F-75005 Paris, France.

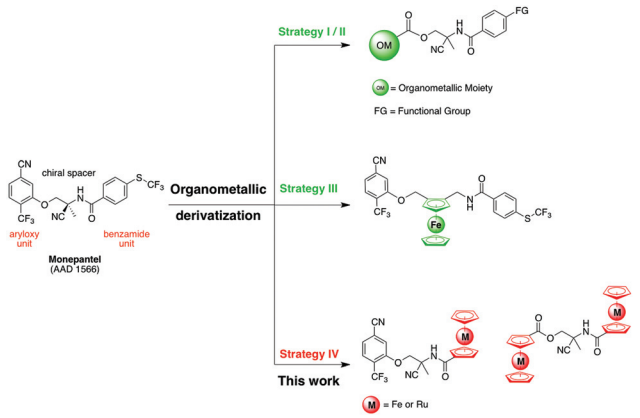

Scheme 1 Schematic representation of previously (green) and newly (red) designed organometallic derivatives of monepantel (AAD 1566) using different strategies. OM = ferrocene, ruthenocene or cymantrene; FG = SCF_3, F, Cl, Br, I, SCH_3, CF_3, OCF_3, $S(O)CF_3$, $S(O)_2CF_3$.

with various organometallic moieties using different strategies (Scheme 1).[19,20] The derivatization of a known organic drug with organometallic moieties has proven to be extremely successful in various fields of medicinal chemistry.[21–35] Ferroquine, a ferrocenyl analogue of the antimalarial drug chloroquine, is one of the best examples of such a derivatization. Thanks to the presence of a ferrocenyl moiety, Ferroquine is active against chloroquine-resistant strains of the malaria parasite, *Plasmodium falciparum* (*P. falciparum*), where the original organic drug chloroquine is inactive.[29,36,37]

In our initial study, we replaced the aryloxy unit of monepantel with organometallic moieties and modified the benzamide part with various functional groups (Scheme 1, Strategy I/II).[19] Subsequently, we replaced the chiral C2 spacer of monepantel by a ferrocenyl moiety that comprised planar chirality with a 1,2-unsymmetric substitution on a cyclopentadienyl ring (Scheme 1, Strategy III).[20]

Extending this work to develop organometallic monepantel derivatives, we report here a new strategy for achieving structurally distinct organometallic-containing monepantel derivatives. First, we kept the aryloxy unit of monepantel unperturbed and substituted the benzamide unit with metallocenes, namely ferrocene and ruthenocene (Scheme 1, Strategy IV). Then, we replaced simultaneously both the aryloxy and the benzamide units using two metallocenyl fragments (Scheme 1, Strategy IV). During the course of present study, we first prepared ferrocenyl monepantel derivatives, since the presence of the ferrocenyl unit might result in additional metal-specific modes of action, such as the production of ROS under physiological conditions. In order to investigate if these redox reactions contribute to the antiparasitic activity of our novel organometallic compounds, we designed ruthenocenyl analogous of the ferrocenyl monepantel derivatives. The replacement of the iron(II) by a ruthenium(II) center is expected to prevent redox mediated ROS production under physiologically relevant conditions.[36,37]

Results and discussion

Synthesis and characterization

The ferrocenyl and ruthenocenyl analogues of monepantel corresponding to Strategy IV were prepared in a two-step reaction procedure as presented in Scheme 2. In order to obtain initial insights into their potential as anthelmintic agents, we focused on the isolation of the organometallic derivatives as racemates rather than as their enantiomerically pure forms.

The syntheses of desired organometallic analogues commenced with the preparation of a 2-amino-2-hydroxymethylproprionitrile (**1**) synthon, following a literature procedure by Gauvry *et al.*[38] The intermediate *N*-(2-cyano-1-hydroxypropan-2-yl)-ferroceneamide (**4a**) was obtained in a moderate yield by reacting **1** with activated ferrocencarboxylic acid (**2**) under basic conditions. Moreover, the same reaction allowed the isolation of a di-ferrocenyl analogue of monepantel, 2-ferroceneamido-2-cyanopropyl ferroceneoate (**5a**), with 11% yield. Compound **4a** was then converted to the desired final compound *N*-(2-cyano-1-(5-cyano-2-(trifluoromethyl)phenoxy)propan-2-yl)ferroceneamide (**6a**) using a Williamson ether synthesis in the presence of NaH and commercially available 3-fluoro-4-(trifluoromethyl)benzonitrile. Compound **6a** was isolated in 26% yield. In addition to the di-ferrocenyl analogue **5a**, another disubstituted organometallic analogue, namely

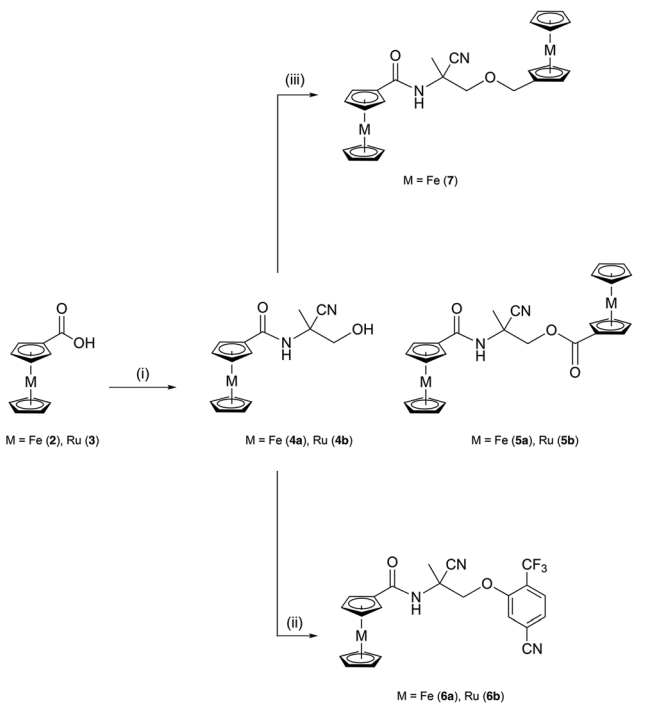

Scheme 2 Reagents and conditions: (i) (a) oxalyl chloride, dry CH_2Cl_2, r.t.; (b) 2-amino-2-hydroxymethylproprionitrile (**1**), NEt_3, dry THF, r.t., o.n., **4a** (50%), **4b** (31%), **5a** (11%), **5b** (19%); (ii) NaH, 3-fluoro-4-(trifluoromethyl)benzonitrile, dry THF, overnight, 0 °C→r.t., **6a** (26%), **6b** (11%); (iii) (ferrocenylmethyl)trimethylammonium iodide, K_2CO_3, 18-crown-6, dry CH_3CN, reflux, 144 h (120 h plus overnight), **7** (43%).

N-(1-(ferrocenyloxy)-2-cyanopropan-2-yl)ferroceneamide (**7**) was also prepared by reacting **4a** with (ferrocenylmethyl)trimethylammonium iodide under basic conditions. By contrast to **5a**, where one of the ferrocenyl units is linked to C2 spacer by an ester functionality, the similar ferrocene unit in **7** is attached to the C2 spacer by an ether functionality. Moreover, we synthesized three ruthenocenyl analogues (**4b**, **5b** and **6b**), which are structurally identical to the ferrocenyl analogues **4a**, **5a** and **6a**. Despite iso-structural, ferrocene and ruthenocene have distinct redox properties, therefore comparison of the biological activity of ferrocenyl and the corresponding ruthenocenyl analogues might shed light on the possible involvement of the redox properties in their activity. The synthetic sequences to obtain the desired ruthenocenyl analogues of monepantel are similar to those of ferrocenyl compounds (see Scheme 2). All novel ferrocenyl and ruthenocenyl analogues of monepantel described here were isolated as racemic mixtures and characterized by ^{1}H, ^{13}C, ^{19}F NMR spectroscopies, ESI-mass spectrometry and IR spectroscopy, and their purities were analyzed by elemental microanalysis.

X-ray crystallography

The molecular structures of four compounds (**4a**/**b**, **6a** and **7**) were further confirmed by X-ray crystallography. Details of the crystallization procedure were given in the Experimental section. The amide unit is coplanar with the cyclopentadienyl ring. The alcohol of compound **4a** is part of a cyclic and a linear hydrogen-bridge network. The R_2^2 (14) cycle[39] is formed by an alcohol hydrogen, making contact with a symmetry ($-x$, $1-y$, $-z$)-related carbonyl oxygen; the corresponding alcohol donates back to the original carbonyl oxygen. Additionally, the same alcohol is an acceptor of a hydrogen bridge from a symmetry related amide nitrogen ($-x$, $1/2+y$, $1/2-z$). The structures of **4a** and **4b** are essentially isostructural, with the major difference being that the Fe–C bond lengths in **4a** are between 2.0293(14) Å and 2.0619(17) Å, whereas the Ru–C bond lengths in **4b** are between 2.155(3) Å and 2.192(3) Å (see Fig. 1). Compound **6a** does not form any "typical" hydrogen bonds, despite the presence of an amide unit (see Fig. 1).

Compound **7** was measured on a synchrotron; it crystallized with two molecules in the asymmetric unit. All cyclopentadienyl rings of the 4 ferrocene units are in an almost perfect eclipsed conformation. One linker starting from the quarternary carbon to the methylene unit next to the cyclopentadienyl ring is disordered in a ratio 3 : 2 (see ESI† for structure).

Biological evaluation

The anthelmintic potentials of our ferrocenyl and ruthenocenyl precursors (**4a**/**b**) and final derivatives **5a**/**b**, **6a**/**b** and **7** were first evaluated on two common parasites of small ruminants, *Haemonchus contortus* (*H. contortus*) and *Trichostrongylus colubriformis* (*T. colubriformis*) using a larval development assay (LDA) (see Experimental section for details). The results are summarized in Table 1. The organic derivatives AAD85, AAD96 and ivermectin were included as controls.[1]

Two of seven metal-based monepantel derivatives tested displayed moderate activities against *H. contortus* and *T. colubriformis*. The final ferrocenyl derivative of Strategy IV (**6a**) and its corresponding ferrocene precursor (**4a**) showed EC_{60} values in a similar range when tested against *H. contortus* 4.90 μg mL^{-1} (15.70 μM) (**4a**) and 4.70 μg mL^{-1} (9.77 μM) (**6a**) and *T. colubriformis* 8.00 μg mL^{-1} (25.63 μM) (**4a**) and 7.00 μg mL^{-1} (14.55 μM) (**6a**). Interestingly, the potencies of both active derivatives (**4a**, **6a**) are approximately twice higher against *H. contortus* compared with *T. colubriformis*. However, the potencies of **4a** and **6a** are lower when compared with the organic controls AAD85 and AAD96, which displayed EC_{100} values of 0.01 μg mL^{-1} (0.022 μM/0.021 μM) and 0.032 μg mL^{-1} (0.07 μM/0.068 μM) against *H. contortus* and *T. colubriformis*, respectively.[1] Importantly, the ruthenocenyl analogues (**4b**, **5b**) of the active ferrocenyl derivatives **4a**, **5a** displayed no activity against *H. contortus* and *T. colubriformis* at the highest concentration evaluated (10 μg mL^{-1}). At this point, it is reasonable to speculate that the iron(II) center in **4a** and **6a** contributes to the production of toxic ROS which could be the reason for the observed anti-parasitic activity of these compounds. Therefore, we evaluated ROS generation using the ferrocene and ruthenocene-containing derivatives in live cells (Fig. 2). Although an assessment of ROS generation in the parasitic nematodes would have been the ideal, however for technical reasons we used a mammalian cervical cancer cell line (HeLa) as model.

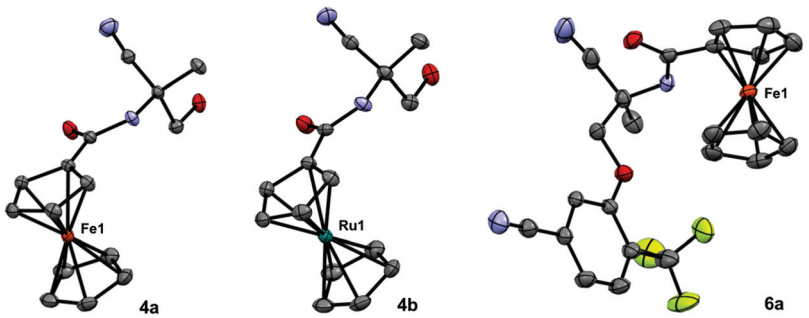

Fig. 1 Molecular structures of **4a**, **4b** and **6a** with atoms shown as thermal ellipsoids (drawn at 50% probability; hydrogen atoms are omitted for clarity).

Table 1 Antiparasitic activity against *Haemonchus contortus*, *Trichostrongylus colubriformis* and *Dirofilaria immitis* and cytotoxicity against HeLa and MRC-5 cells of **4a/b**, **5a/b**, **6a/b**, **7**

	EC_{60} value				EC_{50} value				IC_{50} value	
					D. immitis		*D. immitis*			
	H. contortus		*T. colubriformis*		24 hours		48 hours			
Compound	[μg mL^{-1}]	[μM]	[μg mL^{-1}]	[μM]	[μg mL^{-1}]	[μM]	[μg mL^{-1}]	[μM]	HeLa [μM]	MRC-5 [μM]
4a	4.90	15.70	8.00	25.63	>10.00	>32.04	>10.00	>32.04	>100	>100
5a	>10.00	>19.08	>10.00	>19.08	>10.00	>19.08	>10.00	>19.08	>100	>100
6a	4.70	9.77	7.00	14.55	>10.00	>20.78	>10.00	>20.78	>100	>100
4b	>10.00	>27.98	>10.00	>27.98	>10.00	>27.98	>10.00	>27.98	>100	>100
5b	>10.00	>16.27	>10.00	>16.27	>10.00	>16.27	6.60	10.74	>100	>100
6b	>10.00	>18.99	>10.00	>18.99	6.60	12.54	6.60	12.54	>100	>100
7	>10.00	>19.60	>10.00	>19.60	>10.00	>19.60	>10.00	>19.60	>100	>100
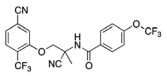 **AAD85**	0.01[a]	0.022[a]	0.032[a]	0.07[a]	2.40	5.25	2.20	4.81	n.d.	n.d.
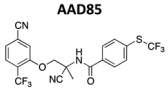 **AAD96**	0.01[a]	0.021[a]	0.032[a]	0.068[a]	n.d.i.	n.d.i.	n.d.i.	n.d.i.	n.d.	n.d.
Ivermectine	0.001[a]	0.001[a]	0.01[a]	0.011[a]	1.00–3.00	1.14–3.43	1.00–3.00	1.14–3.43	n.d.	n.d.
Cisplatin	n.d.	n.d.	n.d.	n.d.	n.d.	n.d.	n.d.	n.d.	9.6 ± 1.2	17.6 ± 4.3

[a] EC_{100} value[1]. n.d.i. = non-disclosable information[4] and n.d. = not determined. EC values are given in μg mL^{-1} as well as in μM. EC values are calculated as a mean of 2 series of triplicated dose responses. Experimental errors are not included as they are too low to influence the overall EC values.

The ROS production in the cells treated with **4a**/**b** and **6a**/**b** (25 μM for 22 h) was quantified using the fluorescent indicator 2′,7′-dichlorofluorescein diacetate (H_2DCFDA). As positive control, *tert*-butyl hydroperoxide (TBH) was included in the same assay. Surprisingly, as shown in Fig. 1, the ROS levels in cells treated with the ferrocenyl compounds (**4a**, **6a**) and the ruthenocenyl compounds (**4b**, **6b**) did not display a significant difference. Moreover, the ROS levels of the cells treated with compounds are comparable to that of the untreated cells.[19]

The results from ROS assay suggest that the differences in anti-parasitic activity between the ferrocene- and ruthenocene-containing organometallic compounds are not related to the production of ROS in cells. However, it has to be pointed out that this is for a timepoint only and that increase in ROS production can be faster or can take longer. The potency of the organometallic monepantel derivatives synthesized using Strategy IV against *H. contortus* and *T. colubriformis* is lower than for the organometallic derivatives from Strategy I/II (best EC_{60} of 1.80 μg mL^{-1}), but superior to those from Strategy III (best EC_{60} of 6.60 μg mL^{-1}).[19,20] Overall, based on knowledge obtained from these structure–activity relationships of organometallic monepantel derivatives, it can be concluded that it is preferable to keep the benzamide part of monepantel unperturbed, while structural modifications can be made to the aryloxy portion for the designing of new derivatives of monepantel to retain anti-parasitic activity against *H. contortus* and *T. colubriformis*.

Previous studies have shown that organometallic derivatization modulates the spectrum of activity of a known organic drug through the addition of metal-specific mode of actions.[37,40] Therefore, we decided to evaluate these compounds further against other parasites.[41,42] The activity of our organometallic-analogues (**4a**/**b**, **5a**/**b**, **6a**/**b** and **7**) of monepantel was evaluated on the canine heartworm, *Dirofilaria immitis* (*D. immitis*). Two ruthenocenyl compounds (**5b**, **6b**) showed moderate activity against microfilariae of this nematode species in a 48 h motility assay with EC_{50} values of 6.60 μg mL^{-1} (10.74 μM (**5b**), 12.54 μM (**6b**)). Interestingly, the corresponding ferrocenyl derivatives **5a** and **6a** are inactive against *D. immitis*. However, once again, **5b** and **6b** are less potent compared to the organic control AAD85, which displays

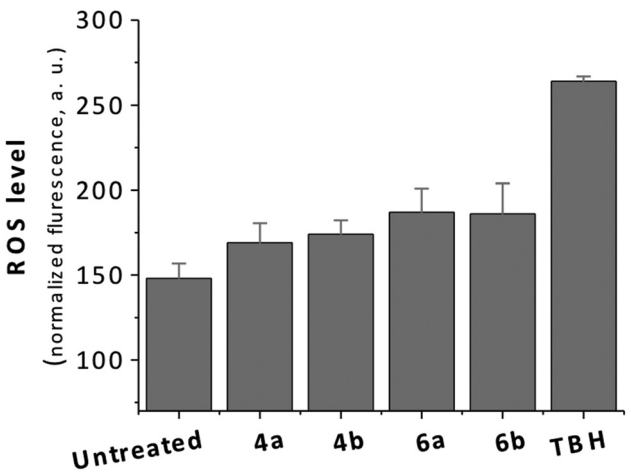

Fig. 2 Level of ROS production in HeLa cells untreated or treated with **4a**, **4b**, **6a** and **6b** after 22 h. THB = *tert*-butyl hydroperoxide.

an EC_{50} value of 2.20 μg mL^{-1} (4.81 μM).[4] In addition to this, we further investigated the activity of the ferrocenyl and ruthenocenyl precursors (**4a**/**b**) and final derivatives **5a**/**b**, **6a**/**b** and **7** on three arthropods *Ctenocephalides felis* (cat flea), *Lucilia cuprina* (blow fly) and *Rhipicephalus sanguineus* (brown dog tick). Unfortunately, none of the compounds synthesized displayed potency at the highest concentration tested on *C. felis* (100 μg mL^{-1}), *L. cuprina* (32 μg mL^{-1}) or *R. sanguineus* (100 μg mL^{-1} and 640 μg mL^{-1}) (Table S1†).

For development of new anti-parasitic compounds, the selectivity of the compounds towards parasites is an important parameter. An ideal anthelmintic should be non-toxic to the mammalian host, while being efficient in killing the parasites. For this purpose, we evaluated the cytotoxicity of the compounds using a cervical cancer cell line (HeLa) and a non-cancerous human lung fibroblast cell line (MRC-5). None of the compounds tested were toxic up to 100 μM (the highest concentration assayed), indicating selectivity of our compounds (**4a**, **6a**) to the nematodes *H. contortus*, *T. colubriformis* and *D. immitis* over mammalian cells.

Conclusion

The extensive use of commercially available broad-spectrum organic anthelmintics has led to a situation where parasites develop resistant to at least one or more available drug classes. With the view of developing a new class of metal-based anthelmintic agents, we synthesized and characterized a series of ferrocene- and ruthenocene-containing organometallic analogues of the anthelmintic drug monepantel. The biological efficacy of all newly synthesized intermediates as well as final analogues (**4a**/**b**, **5a**/**b**, **6a**/**b**, **7**) was assessed in a LDA against *H. contortus* and *T. colubriformis*. Two ferrocenyl derivatives **4a** and **6a** showed moderate efficacy with EC_{60} values between 4.70–8.00 μg mL^{-1} against both nematode species, while the corresponding ruthenocenyl derivatives displayed no activity. The ROS production of both types of organometallic derivatives (**4a**/**b** and **6a**/**b**) was evaluated in an *in vitro* model using the HeLa cervical cancer cell line. However, no significant difference in ROS levels after 22 h was observed between the ferrocenyl (**4a** and **6a**) and ruthenocenyl (**4b** and **6b**) analogues. This unexpected finding might suggest a redox independent mode of action for the anti-parasitic activity of the ferrocenyl derivatives (**4a** and **6a**) although more investigations will need to be performed to confirm this hypothesis. The selectivity of the compounds towards parasites was demonstrated by assessment of their cytotoxicity using a cancer (HeLa) and a non-cancer (MRC-5) cell line.

Experimental section

Materials

All chemicals were of reagent grade quality or better, obtained from commercial suppliers and used without further purification. Solvents were used as received or distilled using standard procedures.[43] All preparations were carried out using standard Schlenk techniques. Thin layer chromatography (TLC) was performed using silica gel 60 F-254 (Merck) plates with detection of spots being achieved by exposure to UV light. Column chromatography was performed using Silica gel 60 (0.040–0.063 mm mesh, Merck). Eluent mixtures are expressed as volume to volume (v/v) ratios. Chlorocarbonyl ferrocene and chlorocarbonyl ruthenocene were synthesized according to literature procedures.[44]

Instrumentation and methods

^{1}H, ^{13}C and ^{19}F NMR spectra were recorded in deuterated solvents on Bruker 400 or 500 MHz NMR at room temperature. The chemical shifts, δ, are reported in ppm (parts per million). The signals from the residual protons of deuterated solvent have been used as an internal reference.[45,46] The abbreviations for the peak multiplicities are as follows: s (singlet), d (doublet), dd (doublet of doublets), t (triplet), q (quartet), m (multiplet), and br (broad). ESI mass spectrometry was performed using a Bruker Esquire 6000 spectrometer. In the assignment of the mass spectra, the most intense peak is listed. UPLC-ESI-MS was performed on a Waters Acquity UPLC System coupled to a Bruker HCTTM, using an Acquity UPLC BEH C18 1.7 μm (2.1 × 50 mm) as a reverse phase column with a flow rate of 0.6 mL min^{-1}. The UV absorption was measured at 254 nm. The runs were performed with a linear gradient of A (acetonitrile (Sigma-Aldrich HPLC grade) and B (distilled water containing 0.02% TFA and 0.05% HCOOC)): t = 0–0.5 min, 5% A; t = 4.0 min, 100% A; t = 5 min, 100% A. High-resolution mass spectrometry were performed on a Bruker ESQUIRE-LC quadrupole ion trap instrument (Bruker Daltonik GmbH, Bremen, Germany), equipped with a combined Hewlett-Packard Atmospheric Pressure Ion (API) source (Hewlett-Packard Co., Palo Alto, CA, USA). The solutions (about 0.1–1 μmol ml^{-1}) were continuously introduced through the electrospray interface with a syringe infusion pump (Cole-Parmer 74900-05, Cole-Parmer Instrument Company, Vernon Hills, Illinois, USA) at a flow rate of 5 μl min^{-1}. The MS-conditions were: nebulizer gas (N_2) 15 psi, dry gas (N_2) 7 min^{-1}, dry temperature 300 °C, capillary voltage 4000 V, end plate 3500 V, capillary exit 100 V, skimmer1 30 V, and trap drive 70. The MS acquisitions were performed at normal resolution (0.6 u at half peak height), under ion charge control (ICC) conditions (10 000) in the mass range from m/z 100 to 2000. To get representative mass spectra, 8 scans were averaged. Infrared spectra were recorded on Perkin-Elmer FTIR spectrometer using KBr pellets. Peak intensities are given as broad (b), very strong (vs), strong (s), medium (m) and weak (w). Elemental microanalyses were performed on a LecoCHNS-932 elemental analyser.

Synthesis

***N*-(2-Cyano-1-hydroxypropan-2-yl)ferroceneamide (4a) and 2-ferroceneamido-2-cyanopropyl ferroceneoate (5a).** Chlorocarbonyl ferrocene (0.648 g, 2.608 mmol) and 2-amino-

2-hydroxymethylproprionitrile (0.261 g, 2.608 mmol) were dissolved in dry THF (100 mL). To this orange reaction solution, NEt_3 (453 μL, 3.26 mmol) was added and the mixture was stirred overnight at room temperature. The solvent was evaporated under reduced pressure. The crude residue was dissolved in CH_2Cl_2 (30 mL), washed with H_2O (2 × 10 mL) and brine (2 × 10 mL). The organic layer was dried over $MgSO_4$, filtered and the solvent was evaporated under reduced pressure. The crude product was purified by column chromatography on silica with hexane : ethyl acetate (4 : 1) as eluent (R_f (**5a**) = 0.69, hexane : ethyl acetate 1 : 1, R_f (**4a**) = 0.30, hexane : ethyl acetate 1 : 1) to afford 2-ferroceneamido-2-cyanopropyl ferroceneoate (**5a**) and *N*-(2-cyano-1-hydroxypropan-2-yl)ferroceneamide (**4a**) as orange solids, respectively. Yield: 11% (**5a**, 0.075 g, 0.143 mmol) and 50% (**4a**, 0.41 g, 1.31 mmol). Data **4a**: IR (KBr, cm^{-1}): 3467s, 3412s, 3103w, 2941w, 2862w, 1635s, 1534m, 1454w, 1377w, 1312m, 1267w, 1201w, 1160w, 1099w, 1056m, 1037w, 1023w, 998w, 911w, 826w, 772w, 710w, 620m, 528w, 499w, 483w, 464w. ^{1}H NMR (400 MHz, d^6-acetone): δ/ppm = 7.12 (s, 1H, N*H*), 5.01 (t, ^3J = 6.4 Hz, 1H, O*H*), 4.85–4.84 (m, 2H, C_5H_4), 4.39–4.38 (m, 2H, C_5H_4), 4.24 (s, 5H, C_5H_5), 4.0–3.93 (m, 1H, CH_2), 3.90–3.86 (m, 1H, CH_2), 1.71 (s, 3H, CH_3). ^{13}C NMR (125 MHz, d^6-acetone): δ/ppm = 170.9, 121.1, 76.1, 71.5, 70.5, 69.5, 69.4, 67.0, 66.9, 53.3, 22.6. ESI-MS: *m*/*z* (%) = 351.02 $[M + K]^+$ (8), 335.04 $[M + Na]^+$ (100), 312.06 $[M]^+$ (52). HR ESI-MS: *m*/*z* (%) = 312.05557, calcd for $C_{15}H_{16}FeN_2O_2$ (M^+) *m*/*z* (%) = 312.05508. Elemental analysis: calcd for $C_{15}H_{16}N_2O_2Fe$ = C, 57.72; H, 5.17; N, 8.97. Found = C, 57.48; H, 5.13; N, 8.69. Data **5a**: IR (golden gate, cm^{-1}): 3368w, 1690m, 1656m, 1520m, 1453w, 1378w, 1288m, 1264w, 1214w, 1164m, 1144m, 1104w, 1027w, 999w, 918w, 827m, 814m, 770m, 741w. ^{1}H NMR (500 MHz, d^6-acetone): δ/ppm = 7.53 (s, 1H, N*H*), 4.88–4.87 (m, 4H, C_5H_4), 4.77 (d, ^2J = 10.8 Hz, 1H, CH_2), 4.82–4.50 (m, 3H, C_5H_4, CH_2), 4.44–4.41 (m, 2H, C_5H_4), 4.27 (s, 5H, C_5H_5), 4.25 (s, 5H, C_5H_5), 1.90 (s, 3H, CH_3). ^{13}C NMR (125 MHz, d^6-acetone): δ/ppm = 171.7, 170.7, 120.21, 75.8, 72.7, 71.7, 71.0, 70.8, 70.6, 69.5, 69.4, 66.9, 51.5, 23.1. ESI-MS: *m*/*z* (%) = 524.1 $[M]^+$ (100). Elemental analysis: calcd for $C_{26}H_{24}N_2O_3Fe_2$ = C 59.58; H 4.62; N 5.34. Found = C 59.51; H 4.52; N 5.25.

***N*-(2-Cyano-1-hydroxypropan-2-yl)ruthenoceneamide (4b) and 2-cyano-2-(ruthenocenecarboxamido)propyl ruthenocnecarboxylate (5b).** Chlorocarbonyl ruthenocene (1.67 g, 6.96 mmol) and 2-amino-2-hydroxymethylproprionitrile (1.05 g, 10.5 mmol) were dissolved in dry THF (50 mL). To this colourless reaction solution NEt_3 (6.8 mL, 50 mmol) was added and the mixture was stirred overnight at room temperature. The solvent was evaporated under reduced pressure. The crude product was purified by column chromatography on silica with hexane : ethyl acetate 7 : 1 → 1 : 7, and the methanol as eluent (R_f (**4b**) = 0.05, hexane : ethyl acetate 7 : 1, R_f (**5b**) = 0.2, methanol) to afford *N*-(2-cyano-1-hydroxypropan-2-yl) ruthenocenamide (**4b**) and 2-cyano-2-(ruthenocenecarboxamido)propyl ruthenocnecarboxylate (**5b**) as pale yellow solids, respectively. Yield: 31% (**4b**, 0.77 g, 2.06 mmol) and 19% (**5b**, 0.81 g, 1.32 mmol). Data **4b**: IR (KBr, cm^{-1}): 3248br, 31122s, 3056w, 2943w, 2887w, 2641w, 2324w, 2241w, 2050w, 1981w, 1720w, 1633s, 1531s, 1455s, 1376s, 1308s, 1130s, 823s. ^{1}H NMR (500 MHz, DMSO): δ/ppm = 7.51 (s, 1H, N*H*), 5.64 (t, ^3J = 6.46 Hz, 1H, O*H*), 5.23–5.22 (m, 2H, C_5H_4), 4.73–4.73 (m, 2H, C_5H_4), 4.59 (s, 5H, C_5H_5), 3.80–3.76 (m, 1H, CH_2), 3.53–3.50 (m, CH_2), 1.54 (s, 3H, CH_3). ^{13}C NMR (125 MHZ, DMSO): δ/ppm = 168.1, 120.5, 79.1, 72.4, 72.3, 71.6, 70.4, 70.3, 64.8, 51.9, 21.7. ESI-MS: *m*/*z* (%) = 359.1 $[M + H]^+$ (100), 259.0 $[M - C_4H_4N_2OH]^+$ (17). Elemental Analysis: calcd for $C_{15}H_{16}O_2N_2Ru$ = C, 50.41; H, 4.51; N, 7.84. Found = C, 50.85; H, 4.44; N, 7.41. Data **5b**: IR (KBr, cm^{-1}): 3320m, 3104w, 2956w, 2651w, 2322w, 2161s, 2053s, 1976s, 1690s, 1656s, 1521s, 1450s, 1373s, 1267s, 1135s, 1035m, 997m, 808s, 759m. ^{1}H NMR (500 MHz, DMSO): δ/ppm = 7.93 (s, 1H, N*H*), 5.27–5.25 (m, 2H, C_5H_3), 5.15–5.13 (m, 2H, C_5H_3), 4.85–4.84 (m, 2H, C_5H_4), 4.76–4.75 (m, 2H, C_5H_4), 4.65 (s, 5H, C_5H_3), 4.59 (s, 5H, C_5H_3), 4.51 (d, ^2J = 10.8, 2H, CH_2), 4.27 (d, ^2J = 10.4, 2H, CH_2), 1.66 (s, 3H, CH_3). ^{13}C NMR (125 MHZ, DMSO): δ/ppm = 168.6, 168.2, 119.2, 78.7, 74.1, 73.3, 72.5, 71.9, 71.6, 71.4, 70.5, 70.3, 64.9, 49.7, 22.1. ESI-MS: *m*/*z* (%) = 639.3 $[M + Na]^+$ (100). Elemental analysis: calcd for $C_{26}H_{24}O_3N_2Ru_2$ = C 50.81; H 3.94; N 4.56. Found = C 50.92; H 3.96; N 4.53.

***N*-(2-Cyano-1-(5-cyano-2-(trifluoromethyl)phenoxy)propan-2-yl)ferroceneamide (6a).** *N*-(2-Cyano-1-hydroxypropan-2-yl)ferroceneamide (**4a**, 0.020 g, 0.064 mmol) was dissolved in dry THF (30 mL). The orange solution was cooled to 0 °C and NaH (0.0018 g, 0.074 mmol) was added. After stirring the reaction mixture for 30 min at 0 °C 3-fluoro-4-(trifluoromethyl)benzonitrile (0.012 g, 0.064 mmol) was added. After stirring the reaction mixture overnight at room temperature, additional NaH (0.0018 g, 0.074 mmol) and 3-fluoro-4-(trifluoromethyl)benzonitrile (0.012 g, 0.064 mmol) were added to the reaction mixture. Another portion of NaH (0.0018 g, 0.074 mmol) was added 2 h later. The reaction was quenched with H_2O (2 mL) and brine (6 mL) and the aqueous layer was extracted with ethyl acetate (3 × 10 mL). The combined organic layers were dried over $MgSO_4$, filtered and the solvent was evaporated under reduced pressure. The crude product was purified by column chromatography on silica with hexane : ethyl acetate (6 : 1) as the eluent (R_f = 0.36, hexane : ethyl acetate 2 : 1) to give *N*-(2-cyano-1-(5-cyano-2-(trifluoromethyl)phenoxy)propan-2-yl)ferroceneamide (**6a**) as an orange solid. Yield: 26% (0.041 g, 0.085 mmol). IR (KBr, cm^{-1}): 3478s, 3414s, 3355s, 2925s, 2851m, 2358m, 2336m, 2240s, 1653s, 1613s, 1574w, 1527m, 1510w, 1465m, 1415m, 1409w, 1373w, 1309m, 1281m, 1261w, 1211w, 1180m, 1141m, 1131m, 1037m, 895w, 841w, 822w, 632w, 606w, 531w, 503w, 486w. ^{1}H NMR (400 MHz, d^6-acetone): δ/ppm = 7.90 (d, ^3J = 8.4 Hz, 1H, arom.), 7.84 (s, 1H, arom.), 7.61 (d, ^3J = 7.6 Hz, 1H, arom.), 7.52 (s, 1H, N*H*), 4.88–4.83 (m, 2H, C_5H_4; 1H, CH_2), 4.67 (d, ^2J = 9.2 Hz, 1H, CH_2), 4.41–4.40 (m, 2H, C_5H_4), 4.22 (s, 5H, C_5H_5), 1.93 (s, 3H, CH_3). ^{13}C NMR (125 MHz, d^6-acetone): δ/ppm = 170.9, 157.0, 129.3, 129.2, 129.2, 129.1, 126.0, 125.1, 123.2, 123.0, 122.9, 119.7, 118.4, 118.0, 75.6, 71.9, 71.7, 71.6, 70.6, 69.6, 69.4, 51.2, 23.0. ^{19}F NMR (282.23 MHz, d^6-acetone): δ/ppm = −63.6. ESI-MS: *m*/*z* (%) = 504.0 $[M + Na]^+$ (100), 985.1 $[2M + Na]^+$ (12). HR ESI-MS: *m*/*z* (%) = 504.05927 calcd for $C_{23}H_{18}F_3FeN_3NaO_2$

([M + Na]$^+$) m/z (%) = 504.05958. Elemental analysis: calcd for $C_{23}H_{18}N_3O_2F_3Fe$ = C 57.40; H 3.77; N 8.73. Found = C 57.62; H 4.01; N 8.38.

***N*-(2-Cyano-1-(5-cyano-2-(trifluoromethyl)phenoxy)propan-2-yl)ruthenoceneamide (6b).** *N*-(2-Cyano-1-hydroxypropan-2-yl) ruthenocenamide (**4b**, 0.150 g, 0.42 mmol) was dissolved in dry THF (30 mL). The colorless solution was cooled to 0 °C and NaH (0.015 g, 0.63 mmol) was added. After stirring the reaction mixture for 30 min at 0 °C 3-fluoro-4-(trifluoromethyl) benzonitrile (0.080 g, 0.42 mmol) was added. After stirring the reaction mixture overnight at room temperature, additional NaH (0.005 g, 0.21 mmol) and 3-fluoro-4-(trifluoromethyl) benzonitrile (0.040 g, 0.21 mmol) were added to the reaction mixture and the reaction was allowed to stir for another 3 h. The reaction was quenched with H_2O (2 mL) and brine (6 mL) and the aqueous layer was extracted with ethyl acetate (3 × 10 mL). The combined organic layers were dried over Na_2SO_4, filtered and the solvent was evaporated under reduced pressure. The crude product was purified by column chromatography on silica with hexane : ethyl acetate 2 : 1 as the eluent (R_f = 0.60) to give *N*-(2-cyano-1-(5-cyano-2-(trifluoromethyl) phenoxy)propan-2-yl)ruthenoceneamide (**6b**) as white solid. Yield: 11% (0.024 g, 0.046 mmol). IR (KBr, cm^{-1}): 3341br, 3076br, 2952w, 2234s, 2165w, 1977s, 1630s, 1575s, 1528s, 1416s, 1285s, 1264s, 1186s, 1132s, 1039s, 816s, 815s, 735s. ^{1}H NMR (500 MHz, d^6-acetone): δ/ppm = 7.89 (d, ^3J = 8.0 Hz, 1H, arom. *H*), 7.80 (s, 1H, arom. *H*), 7.61 (d, ^3J = 8.0 Hz, 1H, arom. *H*), 7.34 (s, 1H, N*H*), 5.20–5.19 (m, 2H, C_5H_4), 4.77 (d, ^3J = 9.5 Hz, 1H, CH_2), 4.71 (s, 2H, C_5H_4), 4.60–4.58 (m, 6H, CH_2 and C_5H_5), 1.87 (s, 3H, CH_3). ^{13}C NMR (125 MHZ, d^6-acetone): δ/ppm = 169.6, 169.5, 157.0, 156.9, 129.3, 129.3, 129.2, 129.2, 127.2, 126.1, 125.1, 123.5, 123.3, 123.0, 122.9, 122.8, 120.7, 119.6, 118.4, 118.4, 118.1, 118.0, 79.9, 79.9, 73.2, 73.2, 72.5, 72.0, 72.0, 71.2, 71.1, 51.2, 51.1, 22.9, 22.9. ^{19}F NMR (470.59 MHz, d^6-acetone): δ/ppm = −63.4. ESI-MS: m/z (%) = 550.0 [M + Na]$^+$ (100). HR ESI-MS: m/z = 528.04751, calcd for $C_{23}H_{18}F_3N_3O_2Ru$ ([M]) m/z = 528.04733; m/z (%) = 550.02942, calcd for $C_{23}H_{18}F_3N_3NaO_2Ru$ ([M + Na]) m/z (%) = 550.02928. Elemental analysis: calcd for $C_{23}H_{21}F_3N_3O_3Ru(H_2O)$ = C 50.73; H 3.70; N 7.72. Found = C 50.61; H 3.40; N 7.51.

***N*-(1-(Ferrocenyloxy)-2-cyanopropan-2-yl)ferroceneamide (7).** *N*-(2-Cyano-1-hydroxypropan-2-yl)ferroceneamide (**4a**, 0.03 g, 0.096 mmol), (ferrocenylmethyl)trimethylammonium iodide (0.065 g, 0.17 mmol), K_2CO_3 (39.8 mg, 0.288 mmol) and 18-crown-6 (0.0076 g, 0.0288 mmol) were dissolved in dry CH_3CN (20 mL) and refluxed (90 °C) for 120 h. Additional (ferrocenylmethyl)trimethylammonium iodide (0.065 g, 0.17 mmol) was added to the reaction and further refluxed overnight. The orange reaction mixture was allowed to reach room temperature. The solvent was evaporated under reduced pressure. The crude residue was redissolved in Et_2O (10 mL) and washed with H_2O (2 × 5 mL) and brine (2 × 5 mL). The organic phase was dried over $MgSO_4$, filtered and the solvent was evaporated under reduced pressure. The crude product was purified by column chromatography on silica using hexane : ethyl acetate 3 : 1 as the eluent (R_f = 0.29) to afford *N*-(1-(ferrocenyloxy)-2-cyanopropan-2-yl)ferroceneamide (**7**) as a yellow solid. Yield: 43% (0.021 g, 0.041 mmol). IR (KBr, cm^{-1}): 3469s, 2929w, 2852w, 1637s, 1518s, 1378w, 1339w, 1305w, 1280w, 1101m, 1008m, 825m, 523m, 502m, 485m. ^{1}H NMR (500 MHz, CD_3CN): δ/ppm = 6.48 (s, 1H, N*H*), 4.73–4.70 (m, 2H, C_5H_4), 4.46 (s, 2H, RCH_2OR), 4.39–4.38 (m, 2H, C_5H_4), 4.32–4.31 (m, 2H, C_5H_4), 4.20 (s, 7H, C_5H_5, C_5H_4), 4.17 (s, 5H, C_5H_5), 3.80 (d, ^3J = 9.3 Hz, 1H, CH_2), 3.70 (d, ^3J = 9.3 Hz, 1H, CH_2), 1.68 (s, 3H, CH_3). ^{13}C NMR (125 MHz, CD_3CN): δ/ppm = 207.9, 171.2, 121.2, 83.9, 75.6, 73.5, 71.9, 70.7, 70.6, 70.5, 69.6, 69.5, 69.5, 69.4, 51.7, 22.9. ESI-MS: m/z (%) = 484.03 [M − CN]$^+$ (12), 510.04 [M]$^+$ (100), 533.00 [M + Na]$^+$ (7). HR ESI-MS: m/z (%) = 510.06882, calcd for $C_{26}H_{26}Fe_2N_2O_2$ ([M + Na]$^+$) m/z (%) = 510.06864. Elemental analysis: calcd for $C_{26}H_{26}N_2O_2Fe_2$ = C 61.21; H 5.14; N 5.49. Found = C 61.06; H 5.20; N 5.31.

Crystallographic studies

Single crystals of **4a** and **7** were grown by slow evaporation of acetonitrile solutions of **4a** or **7** respectively. Single crystals of **4b** were grown by slow evaporation of an dichloromethane solution of **4b**. Single crystals of **6a** were grown by slow evaporation of an acetone solution of **6a**.

Crystallographic data of **4a**, **4b** and **6a** were collected at 183 (2) K with Mo Kα radiation (λ = 0.7107 Å) that was graphite-monochromated on an Oxford Diffraction CCD Xcalibur system with a Ruby detector. Suitable crystals were covered with oil (Infineum V8512, formerly known as Paratone N), placed on a nylon loop that is mounted in a CrystalCap Magnetic™ (Hampton Research) and immediately transferred to the diffractometer. The program suite CrysAlis^{Pro} was used for data collection, multi-scan absorption correction and data reduction.[47] Crystallographic data of **7** were collected at 100(2) K at the PXIII beamline of the SLS synchrotron with a radiation wavelength of 0.71255 Å. The data was integrated with the XDS software[48] and further processed with the CCP4[49] and POINTLESS[50] software. The data has a low completeness because of the one-circle geometry at the beamline and the low symmetry. All structures were solved with direct methods using SIR97[51] and were refined by full-matrix least-squares methods on F^2 with SHELXL-2014.[52] CCDC entries 1501422–1501425 contain the X-ray data of compounds **4a**, **4b**, **6a** and **7**.

Bioassay/s to assess anti-parasitic activity

Some parasites were produced *in vivo* in or on animals. *Haemonchus contortus* and *Trichostrongylus colubriformis* (strongylid nematodes) were maintained in sheep, and *Dirofilaria immitis* (filarial nematodes) in dogs. *Rhipicephalus sanguineus* (tick) was maintained on dogs. All animal experiments were approved by the State of Fribourg, Switzerland, and supervised by the Animal Welfare Officer of Novartis Animal Health. Other parasites, that is, *Ctenocephalides felis* (flea) and *Lucilia cuprina* (fly), were produced *in vitro* and maintained on defibrinated cattle blood. All bioassays were performed by Novartis Animal Health employing industry-standard operating procedures.

Assay to test activity *in vitro* against *Haemonchus contortus* and *Trichostrongylus colubriformis*

This method was conducted as described by Kaminsky *et al.* (2008).[10] In brief, freshly harvested and cleaned nematode eggs were seeded into a 96-well plate containing the test substances to be evaluated for anthelmintic activity. Each compound was tested by serial dilution in order to determine its minimum effective dose. The test compounds were embedded in an agar-based nutritive medium allowing the full development of eggs through to third stage larvae (L3). The plates were incubated for 6 days at 28 °C and 80% relative humidity. Egg hatching and ensuing larval development were recorded to identify a possible nematocidal activity. Efficacy was expressed as a percentage of reduced egg hatch, reduced development of L3, or paralysis and death of larvae of all stages.

Activity *in vitro* against *Dirofilaria immitis*

Microfilariae present in blood from donor dogs chronically infected with *D. immitis* were seeded into 96-well microplates. Individual test compounds were tested by serial dilution to determine their minimum effective doses. The plates were incubated for 48 h at 26 °C and 60% relative humidity. The motility of microfilariae was then recorded to identify any antifilarial activity. Efficacy was expressed as the percentage of reduced motility compared to the control (untreated) and standards. In these assays, a compound needed to exhibit a nematodicidal efficacy of >60% at a concentration of 32 μg ml^{-1} (32 ppm) to qualify for further testing.

Activity *in vitro* against *Ctenocephalides felis*

Oral test. This test was conducted as described by Wade *et al.* (1988) and Zakson-Aiken *et al.* (2001).[53,54] In brief, adult fleas were placed in a suitably formatted microtitration plate, allowing fleas to access and feed on treated blood *via* an artificial feeding system. Each compound was tested by serial dilution to determine its minimum effective doses. Fleas were fed on treated blood for 24 h, after which the compound's effect was recorded. Insecticidal activity was determined on the basis of the number of dead fleas recovered from the feeding system.

Contact test. This test was conducted as described by Wade *et al.* (1988) and Zakson-Aiken *et al.* (2001).[53,54] In brief, adult fleas were distributed into wells of a microplate pre-coated with a serial dilution of the compounds to be evaluated for insecticidal activity. The fleas were left in contact with the compound for 24 h. Insecticidal activity was confirmed upon death of the adult fleas. In these assays, a compound needed to exhibit an insecticidal efficacy of >80% at a concentration of 100 ppm (100 μg ml^{-1}) to qualify for further testing.

Activity *in vitro* against *Rhipicephalus sanguineus* (dog tick)

Immersion test. This test was conducted as described by Lovis *et al.* (2011).[55] In brief, adult *Rhipicephalus sanguineus* were seeded into individual wells of a microtitration plate containing the test substances to be evaluated. Individual test compounds were tested by serial dilution to determine their minimum effective doses. Ticks were left in contact with the test compound for 10 min and then incubated at 28 °C and 80% relative humidity for seven days, during which the test compounds' effects were monitored. Acaricidal activity was confirmed based on the pattern of lethality observed.

Contact (tarsal) test. This test was conducted as described by Lovis *et al.* (2013).[56] In brief, the test was performed by precoating wells of a 96-well microliter plate with a serial dilution of compound, allowing the evaluation of anti-parasitic activity by contact with ticks. Adult ticks were then distributed to individual wells of the plate and incubated at 28 °C and 80% relative humidity for seven days, during which the test compound's effect was monitored. Acaricidal activity was confirmed upon death of the adult ticks.

Determination of ROS level

The assay was performed following a procedure published by our group with slight modification.[57] Briefly, HeLa cells (8000 in 100 μL medium per well) were seeded in a 96 well plate (black, clear flat bottom from corning). Next day, the media was aspirated and 200 μM fresh media containing **4a**, **4b**, **6a** or **6b** (freshly prepared stock solution in DMSO, after dilution with culture medium final concentration of DMSO ≤0.3%, 25 μM exposure concentration) was added. Cells were then incubated at 37 °C incubator for 22 h. The medium was then removed, washed with 150 μL PBS and then 150 μL solution of H2DCFDA (final concentration 20 μM) in serum free medium was added and incubated for 40 min in dark. The fluorescence generated by intracellular ester cleavage followed by oxidation of H2DCFDA by intracellular ROS was quantified at 528 nm emission with 485 nm excitation wavelength in a SpectraMax M5 microplate reader. For the positive control TBH, 100 μM concentration and 6 h incubation time was used. After quantification of the ROS, cell viability on HeLa cells was determined to quantify the potential decrease in cellular mass due to treatment with different compounds. The media was aspirated and cells were washed with 150 μL PBS. Afterwards, 100 μL 0.4% formaldehyde in PBS was added and cells were allowed to fix for 20 min at room temperature. The formaldehyde solution was aspirated and cells were washed with 150 μL PBS. 0.02% crystal violet (CV) solution in PBS was then added (100 μL per well) and incubated at room temperature for 30 min. The CV solution was then aspirated, washed with 150 μL of distilled water and dried overnight. Next day, 180 μL 80% ethanol was added to each well and the plates were gently shaken on a rocker for 2–3 h and were read at 570 nm in a SpectraMax M5 microplate reader. The results expressed as mean and standard error of six replicates, corrected for the viable cell population.

Cell culture

Human cervical carcinoma cells (HeLa) were cultured in DMEM (Gibco) supplemented with 5% fetal calf serum (FCS, Gibco), 100 U ml^{-1} penicillin, 100 μg ml^{-1} streptomycin at 37 °C and 5% CO_2. The normal human fetal lung fibroblast

MRC-5 cell line was maintained in F-10 medium (Gibco) supplemented with 10% FCS (Gibco), penicillin (100 U ml^{-1}), and streptomycin (100 μg ml^{-1}).

Cytotoxicity studies

Cytotoxicity studies were performed on two different cell lines, namely HeLa, and MRC-5, by a fluorometric cell viability assay using Resazurin (Promocell GmbH). Briefly, one day before treatment, cells were seeded in triplicates in 96-well plates at a density of 4×10^3 cells per well for HeLa and 7×10^3 for MRC-5 in 100 μl growth medium. Upon treating cells with increasing concentrations of organometallic-monepantel derivatives for 48 h, the medium was removed, and 100 μl complete medium containing Resazurin (0.2 mg ml^{-1} final concentration) were added. After 4 h of incubation at 37 °C, fluorescence of the highly red fluorescent product Resorufin was quantified at 590 nm emission with 540 nm excitation wavelength in a SpectraMax M5 microplate reader.

Abbreviations

AADs	Amino-acetonitrile derivatives
C. felis	*Ctenocephalides felis*
D. immitis	*Dirofilaria immitis*
ESI-MS	Electrospray ionisation-mass spectrometry
H. contortus	*Haemonchus contortus*
H2DCFDA	2′,7′-Dichlorofluorescein diacetate
LDA	Larval development assay
L. cuprina	*Lucilia cuprina*
nAChR	Nicotinic acetylcholine receptor
o.n.	Overnight
P. falciparum	*Plasmodium falciparum*
ROS	Reactive oxygen species
R. sanguineus	*Rhipicephalus sanguineus*
r.t.	Room temperature
SAR	Structure activity relationship
TBH	*tert*-Butyl hydroperoxide
T. colubriformis	*Trichostrongylus colubriformis*.

Acknowledgements

This work was financially supported by the Swiss National Science Foundation (Professorships No. PP00P2_133568 and PP00P2_157545 to G. G.), the University of Zurich (G. G., S. F.), the Stiftung für wissenschaftliche Forschung of the University of Zurich (G. G., S. F.), the Novartis Jubilee Foundation (G. G.), the Kurt u. Senta Hermann Stiftung (S. F.) and the Swiss Government Excellence Scholarship for Postdoctoral Researcher (R. L.). R. B. G.'s research program is supported by the Australian Research Council (ARC), the National Health and Medical Research Council (NHMRC), Melbourne Water Corporation, Yourgene Bioscience and the Alexander von Humboldt Foundation and The University of Melbourne. R. B. G. is a grateful recipient of Professorial Humboldt Research Awards. The authors would like to thank Dr Jacques Bouvier (Novartis Animal Health, St-Aubin, Switzerland) and Dr Noëlle Gauvry (Novartis Animal Health, Basel, Switzerland) for their help with the biological assays.

References

1 P. Ducray, N. Gauvry, F. Pautrat, T. Goebel, J. Fruechtel, Y. Desaules, S. S. Weber, J. Bouvier, T. Wagner, O. Froelich and R. Kaminsky, *Bioorg. Med. Chem. Lett.*, 2008, **18**, 2935–2938.
2 R. Kaminsky, L. Rufener, J. Bouvier, R. Lizundia, S. Schorderet Weber and H. Sager, *Vet. Parasitol.*, 2013, **195**, 286–291.
3 C. P. Gordon, L. Hizartzidis, M. Tarleton, J. A. Sakoff, J. Gilbert, B. E. Campbell, R. B. Gasser and A. McCluskey, *MedChemComm*, 2014, **5**, 159–164.
4 For legal issues the efficacy of AAD96 cannot be disclosed.
5 R. M. Kaplan and A. N. Vidyashankar, *Vet. Parasitol.*, 2012, **186**, 70–78.
6 R. M. Kaplan, *Trends Parasitol.*, 2004, **20**, 477–481.
7 S. B. Howell, J. M. Burke, J. E. Miller, T. H. Terrill, E. Valencia, M. J. Williams, L. H. Williamson, A. M. Zajac and R. M. Kaplan, *J. Am. Vet. Med. Assoc.*, 2008, **233**, 1913–1919.
8 L. L. Mortensen, L. H. Williamson, T. H. Terrill, R. A. Kircher, M. Larsen and R. M. Kaplan, *J. Am. Vet. Med. Assoc.*, 2003, **23**, 495–500.
9 C. Epe and R. Kaminsky, *Trends Parasitol.*, 2013, **29**, 129–134.
10 R. Kaminsky, P. Ducray, M. Jung, R. Clover, L. Rufener, J. Bouvier, S. S. Weber, A. Wenger, S. Wieland-Berghausen, T. Goebel, N. Gauvry, F. Pautrat, T. Skripsky, O. Froelich, C. Komoin-Oka, B. Westlund, A. Sluder and P. Maser, *Nature*, 2008, **452**, 176–180.
11 L. Rufener, J. Keiser, R. Kaminsky, P. Mäser and D. Nilsson, *PLoS Pathog.*, 2010, **6**, e1001091.
12 R. Baur, R. Beech, E. Sigel and L. Rufener, *Mol. Pharmacol.*, 2015, **87**, 96–102.
13 L. Rufener, N. Bedoni, R. Baur, S. Rey, D. A. Glauser, J. Bouvier, R. Beech, E. Sigel and A. Puoti, *PLoS Pathog.*, 2013, **9**, e1003524.
14 L. Rufener, P. Maeser, I. Roditi and R. Kaminsky, *PLoS Pathog.*, 2009, **5**, e1000380.
15 R. Van den Brom, L. Moll, C. Kappert and P. Vellema, *Vet. Parasitol.*, 2015, **209**, 278–280.
16 A. Mederos, Z. Ramos and G. Banchero, *Parasites Vectors*, 2014, **7**, 598.
17 A. S. Cezar, G. Toscan, G. Camillo, L. A. Sangioni, H. O. Ribas and F. S. F. Vogel, *Vet. Parasitol.*, 2010, **173**, 157–160.
18 I. Scott, W. E. Pomroy, P. R. Kenyon, G. Smith, B. Adlington and A. Moss, *Vet. Parasitol.*, 2013, **198**, 166–171.
19 J. Hess, M. Patra, L. Rangasamy, S. Konatschnig, O. Blacque, A. Jabbar, P. Mac, E. M. Jorgensen, R. B. Gasser and G. Gasser, *Chem. – Eur. J.*, 2016, DOI: 10.1002/chem.201602851.

20 J. Hess, M. Patra, V. Pierroz, B. Spingler, A. Jabbar, S. Ferrari, R. B. Gasser and G. Gasser, *Organometallics*, 2016, **35**, 3369–3377.
21 G. Gasser and N. Metzler-Nolte, *Curr. Opin. Chem. Biol.*, 2012, **16**, 84–91.
22 G. Gasser, I. Ott and N. Metzler-Nolte, *J. Med. Chem.*, 2011, **54**, 3–25.
23 G. Jaouen and N. Metzler-Nolte, *Topics in Organometallic Chemistry*, Springer, 2010.
24 C. G. Hartinger and P. J. Dyson, *Chem. Soc. Rev.*, 2009, **38**, 391–401.
25 P. C. A. Bruijnincx and P. J. Sadler, *Curr. Opin. Chem. Biol.*, 2008, **12**, 197–206.
26 C. Biot, G. Glorian, L. A. Maciejewski, J. S. Brocard, O. Domarle, G. Blampain, P. Millet, A. J. Georges, H. Abessolo, D. Dive and J. Lebibi, *J. Med. Chem.*, 1997, **40**, 3715–3718.
27 C. Biot and D. Dive, in *Medicinal Organometallic Chemistry*, ed. G. Jaouen and N. Metzler-Nolte, Springer-Verlag, Heidelberg, 2010, vol. 32, pp. 155–193.
28 C. Biot, W. Castro, C. Y. Botte and M. Navarro, *Dalton Trans.*, 2012, **41**, 6335–6349.
29 D. Dive and C. Biot, *ChemMedChem*, 2008, **3**, 383–391.
30 R. Rubbiani, O. Blacque and G. Gasser, *Dalton Trans.*, 2016, **45**, 6619–6626.
31 M. Patra, G. Gasser, M. Wenzel, K. Merz, J. E. Bandow and N. Metzler-Nolte, *Organometallics*, 2010, **29**, 4312–4319.
32 M. Patra, G. Gasser, A. Pinto, K. Merz, I. Ott, J. E. Bandow and N. Metzler-Nolte, *ChemMedChem*, 2009, **4**, 1930–1938.
33 M. Patra, K. Ingram, V. Pierroz, S. Ferrari, B. Spingler, R. B. Gasser, J. Keiser and G. Gasser, *Chem. – Eur. J.*, 2013, **19**, 2232–2235.
34 M. Patra, K. Ingram, V. Pierroz, S. Ferrari, B. Spingler, J. Keiser and G. Gasser, *J. Med. Chem.*, 2012, **55**, 8790–8798.
35 M. Patra, K. Ingram, A. Leonidova, V. Pierroz, S. Ferrari, M. N. Robertson, M. H. Todd, J. Keiser and G. Gasser, *J. Med. Chem.*, 2013, **56**, 9192–9198.
36 F. Dubar, T. J. Egan, B. Pradines, D. Kuter, K. K. Ncokazi, D. Forge, J.-F. O. Paul, C. Pierrot, H. Kalamou, J. Khalife, E. Buisine, C. Rogier, H. Vezin, I. Forfar, C. Slomianny, X. Trivelli, S. Kapishnikov, L. Leiserowitz, D. Dive and C. Biot, *ACS Chem. Biol.*, 2011, **6**, 275–287.
37 N. Chavain, H. Vezin, D. Dive, N. Touati, J.-F. Paul, E. Buisine and C. Biot, *Mol. Pharmaceutics*, 2008, **5**, 710–716.
38 N. Gauvry, T. Goebel, P. Ducray, F. Pautrat, R. Kaminsky and M. Jung, WO05/044784, 2005; *Chem. Abstr.*, 2005, **142**, 481750.
39 J. Bernstein, R. E. Davis, L. Shimoni and N. L. Chang, *Angew. Chem., Int. Ed. Engl.*, 1995, **34**, 1555–1573.
40 S. Top, A. Vessières, G. Leclercq, J. Quivy, J. Tang, J. Vaissermann, M. Huché and G. Jaouen, *Chem. – Eur. J.*, 2003, **9**, 5223–5236.
41 C. Biot, G. Glorian, L. A. Maciejewski and J. Brocard, *J. Med. Chem.*, 1997, **40**, 3715–3718.
42 G. Jaouen, S. Top, A. Vessières, G. Leclercq and M. J. McGlinchey, *Curr. Med. Chem.*, 2004, **11**, 2505–2517.
43 W. L. F. Armarego and D. D. Perrin, *Purification of Laboratory Chemicals*, Butterworth-Heinemann, Oxford, UK, 4th edn, 1996.
44 D. P. Cormode, A. J. Evans, J. J. Davis and P. D. Beer, *Dalton Trans.*, 2010, **39**, 6532–6541.
45 H. E. Gottlieb, V. Kotlyar and A. Nudelman, *J. Org. Chem.*, 1997, **62**, 7512–7515.
46 G. R. Fulmer, A. J. M. Miller, N. H. Sherden, H. E. Gottlieb, A. Nudelman, B. M. Stoltz, J. E. Bercaw and K. I. Goldberg, *Organometallics*, 2010, **29**, 2176–2179.
47 Agilent Technologies, Journal, 2014, Xcalibur CCD system.
48 W. Kabsch, *Acta Crystallogr., Sect. D: Biol. Crystallogr.*, 2010, **66**, 125–132.
49 S. Bailey, *Acta Crystallogr., Sect. D: Biol. Crystallogr.*, 1994, **50**, 760–763.
50 P. R. Evans, *Acta Crystallogr., Sect. D: Biol. Crystallogr.*, 2011, **67**, 282–292.
51 A. Altomare, M. C. Burla, M. Camalli, G. L. Cascarano, C. Giacovazzo, A. Guagliardi, A. G. G. Moliterni, G. Polidori and R. Spagna, *J. Appl. Crystallogr.*, 1999, **32**, 115–119.
52 G. M. Sheldrick, *Acta Crystallogr., Sect. C: Cryst. Struct. Commun.*, 2015, **71**, 3–8.
53 M. Zakson-Aiken, L. M. Gregory, P. T. Meinke and W. L. Shoop, *J. Med. Entomol.*, 2001, **38**, 576–580.
54 S. E. Wade and J. R. Georgi, *J. Med. Entomol.*, 1988, **25**, 186–190.
55 L. Lovis, J. L. Perret, J. Bouvier, J. M. Fellay, R. Kaminsky, B. Betschart and H. Sager, *Vet. Parasitol.*, 2011, **182**, 269–280.
56 L. Lovis, M. C. Mendes, J. L. Perret, J. R. Martins, J. Bouvier, B. Betschart and H. Sager, *Vet. Parasitol.*, 2013, **191**, 323–331.
57 R. Rubbiani, T. N. Zehnder, C. Mari, O. Blacque, K. Venkatesan and G. Gasser, *ChemMedChem*, 2014, **9**, 2781–2790.